Underwater acoustic channel characterisation for medium-range shallow water communications

Mandar Chitre, John Potter, Ong Sim Heng

National University of Singapore, 12a Kent Ridge Road, Singapore 119223
mandar@arl.nus.edu.sg, johnp@arl.nus.edu.sg, eleongsh@nus.edu.sg

ABSTRACT

The ability to effectively communicate underwater has numerous applications for researchers, marine commercial operators and defence organizations. As electromagnetic waves cannot propagate over long distances in seawater, acoustics provides the most obvious choice of channel. Although acoustics has been used effectively for point-to-point communications in deep-water channels, acoustics has had limited success for horizontal transmissions in shallow water. Time-varying multi-path propagation and non-Gaussian noise are two of the major factors that limit acoustic communication performance in shallow water.

Although it is known that medium-range shallow water propagation is dominated by time-varying multi-path arrivals, very few measurements of the variability of the multi-path structure are available. In this paper, we present channel measurements made in a shallow water channel (depth 15-20m) up to a range of 1km. An analysis of the temporal variability of the arrival structure is presented.

Most communication systems make the assumption that the noise is additive and Gaussian. Snapping shrimp dominate the ambient noise spectrum above a few kHz in warm shallow waters. It is known that snapping shrimp noise is impulsive and highly non-Gaussian. These noise characteristics need to be taken into account when designing communication systems if robust and near-optimal performance is desired. An analysis of the ambient noise characteristics from some warm shallow water channels is also presented.

I. INTRODUCTION

Acoustic communications in shallow waters had been a difficult problem due to the unique channel characteristics of the underwater acoustic channel. Fading and multipath arrivals are believed to be key issues in such channels [1][2]. Powerful receiver algorithms coupled with decision feedback equalizers (DFE) and second order phase locked loops (PLL) enabled phase coherent communications to achieve rates up to 10 kbps in medium range shallow water channels [3][4]. More recently, data rates of 20 kbps have been reported in Woods Hole harbour [2] while data rates of 15 kbps have been reported in the Baltic Sea [5].

The medium range very shallow water channel, commonly found in coastal regions such as Singapore waters, is believed to be an extremely challenging channel due to time-varying multipath arrivals as well as high levels of ambient noise due to shipping and snapping shrimp. Although most communication systems assume Gaussian noise, it is known that the energy distribution of snapping shrimp dominated ambient noise is highly non-Gaussian [6]. Modems that have yielded good data rates in other shallow water channels have not been able to perform as well in Singapore waters. To understand the poor performance of acoustic communication systems, we explored the noise characteristics and time variability of multipath arrivals in these waters.

II. AMBIENT NOISE

A. Noise Statistics

Low frequency ambient noise in Singapore waters is dominated by shipping and reclamation noise while high frequencies are dominated by snapping shrimp noise [7]. As the channel of interest is a medium range channel, we are primarily interested in the higher frequency band from 10 kHz to about 80 kHz. Based on data sets from different shallow water regions of the world, the energy distribution of snapping shrimp noise in this band has been shown to be approximately log-Normal [6]. Although this suggests a non-Gaussian distribution for the dynamic pressure of the ambient noise, this seems to have received little attention from designers of acoustic modems.

Fig. 1 shows a Normal Probability Plot of the pressure distribution of ambient noise in Singapore waters. The scale on the plot is designed such that a Gaussian distribution would appear linear on the plot. The deviation from linearity clearly shows that the distribution is heavy tailed i.e. the high amplitudes of pressure are much more likely than in a Gaussian distribution. This is not surprising, as the noise produced by snapping shrimp is known to be impulsive [8].

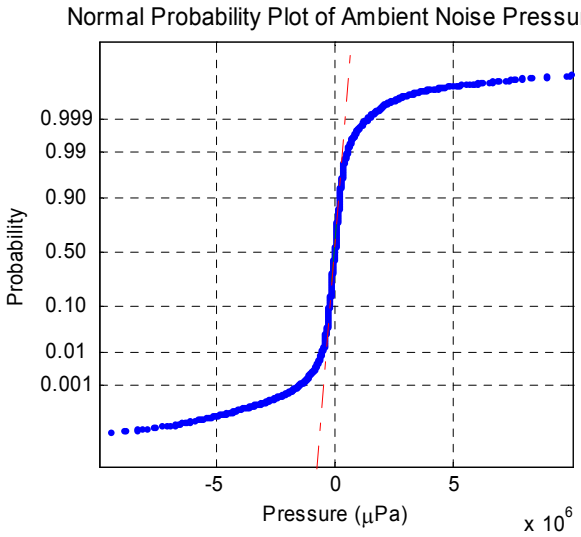

Fig. 1. A Normal Probability Plot of acoustic pressure of ambient noise recorded in Singapore waters shows severe deviation (heavy tails) from Gaussian distribution

Non-Gaussian noises have been commonly modelled using Gaussian mixture, generalized Gaussian or Gaussian double exponential distributions [9]. However, none of these distributions yielded good fits to the observed ambient noise.

A family of distributions known as the *stable* distributions has been shown to be a powerful tool in the study of heavy tailed phenomenon [10]. Stable distributions are a direct generalization of the Gaussian distribution and include Gaussian as a limiting case. A parameter known as the characteristic exponent ($0 < \alpha \leq 2$) of the distribution controls the heaviness of its tails. A value of 2 for α denotes the limiting Gaussian distribution while smaller values of α indicate heavier tails or more impulsive distributions.

An important subclass of the stable distributions is the symmetric α-stable (SαS) distribution. This subclass yielded a good fit to all the ambient noise samples that we tested. To estimate the distribution parameters for a good fit, we used the fractile based estimators developed by McCulloh [11] and Fama and Roll [12]. Values of α between 1.5 and 1.6 yielded a good fit for most of the observed ambient noise. A SαS and Gaussian best fit to an ambient noise sample is shown in Fig. 2. Although it appears that a narrower Gaussian probability density function (PDF) would fit the central region better, narrowing of the PDF worsens the fit in the long tail regions and consequently increases the total error.

B. Linear Correlator

In presence of Gaussian noise, the linear correlator is an optimal detector for a known signal. Many communication schemes use this detector in the form of a matched filter.

The linear correlator, scaled such that its output is an optimal estimate of the signal strength is given by:

$$\Lambda = \frac{\sum_t x(t)s(t)}{\sum_t s(t)^2} \tag{1}$$

where $s(t)$ is the signal to be detected and $x(t)$ is the observed data.

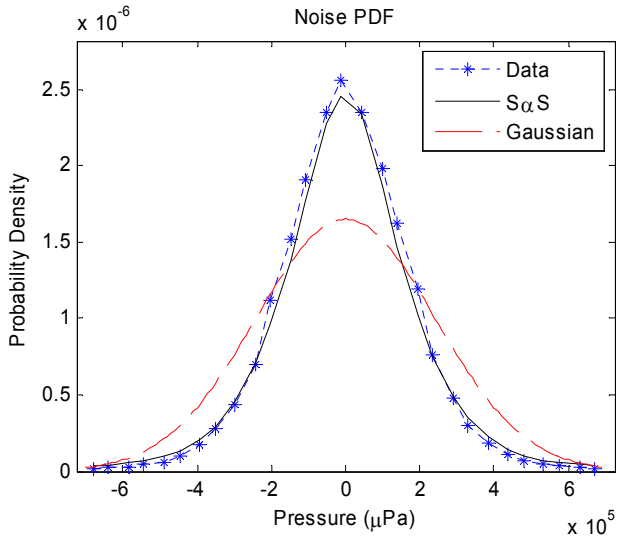

Fig. 2. The SαS probability distribution yields a good fit to observed ambient noise data

C. Maximum Likelihood Estimator

In the presence of SαS noise, the linear correlator is no longer optimal. In fact, a uniformly optimal detector does not exist. Locally optimal detectors for detecting weak signals in SαS noise have been developed [10]. However, these detectors are not optimal for stronger signals, which may still be too weak to detect using the sub-optimal linear correlator.

A maximum likelihood (ML) detector can be developed by maximizing the likelihood of noise based on the knowledge of the noise probability density function (PDF). Maximizing the log-likelihood is equivalent to maximizing the likelihood. The log-likelihood function and the ML estimates are given by:

$$\begin{aligned} L(A) &= \sum_t \log\{f_n[x(t) - As(t)]\} \\ \hat{L} &= \max_A L(A) \\ \hat{A} &= \arg\max_A L(A) \end{aligned} \tag{2}$$

where $f_n(\ldots)$ is the PDF of the noise and A is a parameter to be optimised. The maximum log-likelihood $\hat{L}$ may be used as a detection statistic while $\hat{A}$ is an optimal estimate of signal strength.

Unfortunately, the SαS distribution does not have a closed form expression for its PDF. Although efficient numerical methods have been developed to compute the SαS PDF [13], the lack of a closed form expression requires a numerical search for ML detection. This makes it computationally too complex to be of practical use in a communication system.

D. Sign Correlator

A simple modification to the linear correlator yields a sign correlator, which is known to be an optimal detector in double exponential density noise. The sign correlator has been reported to have robust performance in many other types of non-Gaussian noise [9]. Hence we selected it as a candidate detector in snapping shrimp dominated noise and studied its performance.

The sign correlator, scaled such that a perfect correlation yields a value of 1 is given by:

$$\Lambda = \frac{\sum_t \mathrm{sgn}[x(t)]s(t)}{\sum_t |s(t)|} \tag{3}$$

where $s(t)$ is the known signal, $x(t)$ is the observed data and sgn[…] is the signum function.

A disadvantage of the sign correlator is that the output statistic cannot be used as an estimate of the signal strength. If such an estimate is desired, the sign correlator may be used in conjunction with a ML estimator; the sign correlator would detect the signal and the ML estimator would then estimate its strength. We used this scheme to analyse data from channel response measurements, which are presented later in this paper.

E. Detection Performance in SαS Noise

To compare the performances of the linear correlator, the ML detector and the sign correlator, we created synthetic data by adding ambient noise samples to a known spread spectrum signal of varying strength. The detectors

were applied to the synthetic data to compare performance. For each of the signal strengths, 50,000 iterations with different ambient noise samples were performed to get an estimate of detection probability. All detections were performed with a constant false alarm rate (CFAR) of 0.001.

As the variance of a SαS distribution is infinite, we adopted a signal-to-dispersion ratio (E_0/N_0) as a measure of signal-to-noise ratio (SNR). Dispersion is a parameter which controls the width of the SαS distribution, in a similar way as variance controls the width of a Gaussian distribution. E_0/N_0 is used as measure of SNR in SαS signal processing by many researchers [10].

Fig. 3 shows the results of the Monte-Carlo simulations of detection performance in snapping shrimp dominated ambient noise. The linear correlator performance is much lower than the other detectors. The MLE and the log-likelihood curves are based on the ML detector. The MLE curve uses the estimate of the signal strength to make its decision while the Log-likelihood curve uses the log-likelihood function as the detection statistic. The sign correlator performance is only slightly inferior to the ML estimator. Given its good performance, simplicity of implementation and low computational complexity, it is an ideal detector in heavy-tailed ambient noise.

III. MULTIPATH STRUCTURE

A. Experimental Setup

An experiment was conducted in February 2004 to measure the time-variability of the impulse response of the very shallow acoustic channel in Singapore waters. The location chosen allowed measurements up to 1 km range in a relatively flat area with an average depth of about 15 m. Transmissions were made from an omni-directional transducer located at the bottom of a 4 m pole mounted on the bow of a research vessel as shown in Fig. 4. The signal was received using a hydrophone located at the bottom of a 4 m pole mounted on the side of an anchored barge. The signal was sampled at 250 kSa/s and stored for later analysis. The research vessel moved to various locations and made transmissions. GPS coordinates of the vessel and the barge were noted for range computation.

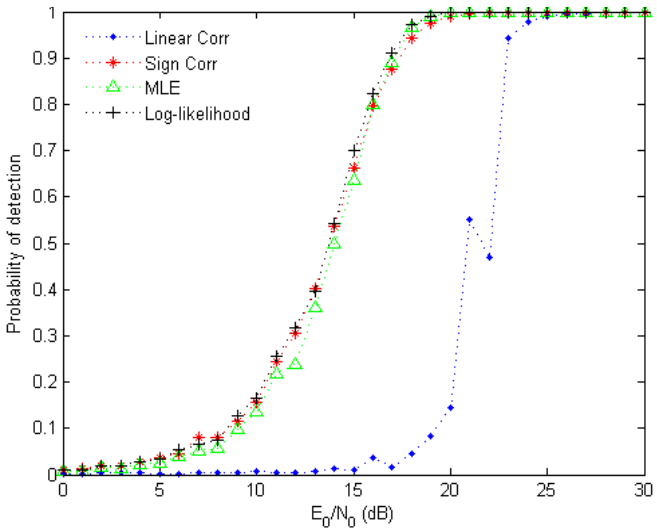

Fig. 3. Results of Monte-Carlo simulation to test various detectors in snapping-shrimp dominated ambient noise

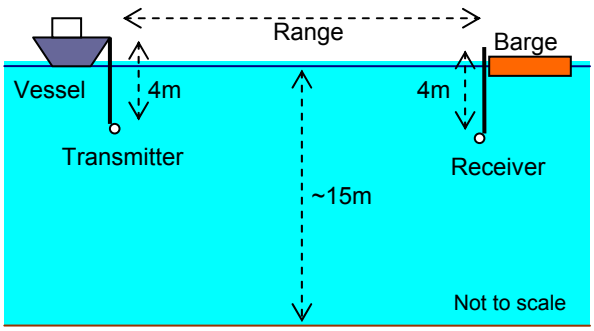

Fig. 4. Experimental setup for channel measurements

The signal used was a 30 ms direct sequence spread spectrum BPSK signal with a bandwidth of 40 kHz centred around 40 kHz. The signal was repeated 100 times at a rate of 10 Hz at each location of the research vessel. The different transmission locations corresponded to ranges of 50 m, 100 m, 550 m, 780 m and 1020 m. The measurements were made in relatively calm weather over a period of an hour.

B. Signal Processing

The recorded signals were post-processed to obtain estimates of the time-variability of the multipath structure of the channel. The processing involved several steps:

1. The recorded data was band-pass filtered with a FIR filter with a pass-band from 20 kHz to 60 kHz to remove all out-of-band noise.
2. The template signal was filtered with the known frequency response of the transducer, corrected for the estimated frequency-dependent absorption by sea-water.
3. The arrivals of the signals were detected using the sign correlator.
4. The first arrival of each transmitted signal was identified based on known transmission rate. The multipath delays of later arrivals were computed relative to the first arrival.
5. The multipath arrival structure thus obtained was then analyzed. The results of the analysis are presented in the following sections.
6. The fading behaviour of the signal was determined using the ML estimator. The SαS distribution assumed for the ML estimator was calibrated using ambient noise samples recorded at the experimental site.

C. Results & Discussion

1) Short Range

At short range (50 m and 100 m), a ray model explained the observed data well. The direct arrival, surface reflected arrival and the bottom reflected arrival could be clearly distinguished as seen in Fig. 5. The arrival timings matched those predicted by simple ray models well. The surface reflected arrival usually suffered very little loss, whereas the bottom reflected arrival was 10-15 dB lower than the direct arrival. Consistent with models of sea bed reflection, the bottom loss at 50 m was higher than that at 100 m. Weaker reflections were often seen at delays corresponding to multiple surface-bottom interactions. Additional reflections, believed to be from nearby objects were occasionally observed.

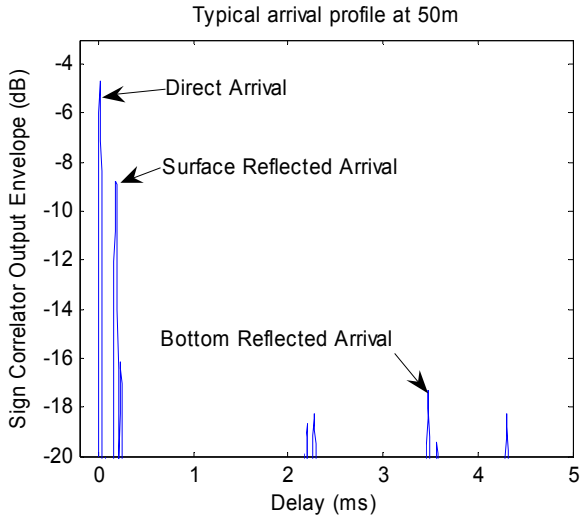

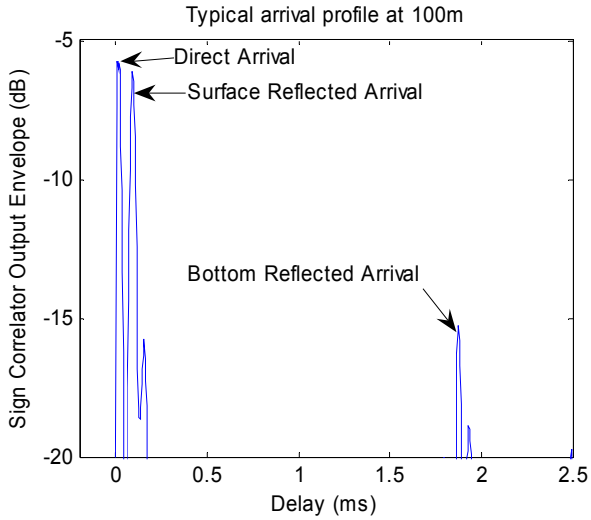

Fig. 5. Multipath arrival structure at 50 m and 100 m range

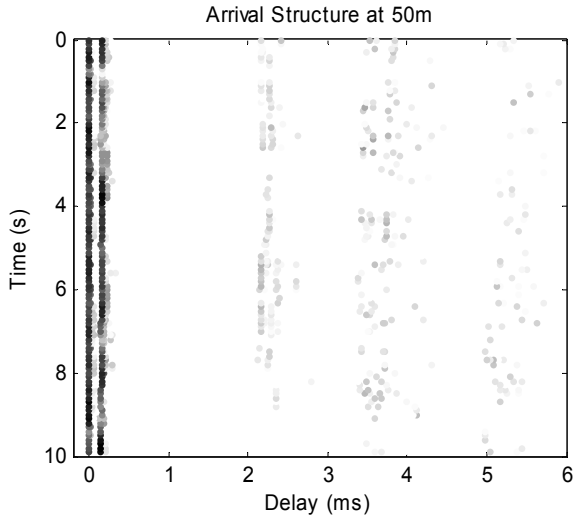

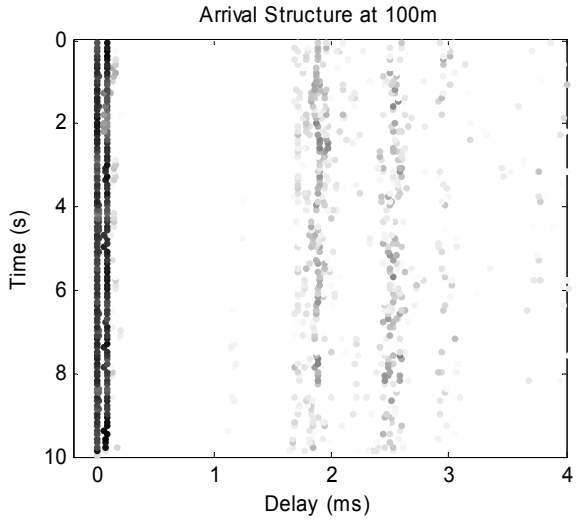

Fig. 6. Multipath arrival structure for 100 signal transmissions at 50 m and 100 m range

To understand the time variability of the multipath structure, it is necessary to observe the arrival structure of all 100 transmissions. Fig. 6 shows a plot of the arrival structure of all transmissions, with the transmission time on the y-axis, the delay on the x-axis and the darkness of each point showing the arrival strength.

At 50m, the direct and surface reflected arrivals are seen clearly. The surface reflected arrival shows very little variability in arrival time. However, it occasionally fades. The direct arrival and surface reflection are closely followed by secondary reflections with much lower amplitudes and are subject to more fading. The bottom reflected arrival is seen at about 3.6 ms. This arrival shows considerable variability in time and amplitude. An additional reflection from an unknown object is seen at about 2.3 ms. This arrival has slower variations is both arrival time and amplitude.

At 100m, the surface reflected arrival is stable in arrival time and also more stable in amplitude. The bottom reflected arrival is seen at about 1.8 ms. This is much more stable in time and amplitude and shows slow variation. The variation show a wavy pattern, which may arise from the movement of the barge and the boat with respect to the bottom. A model-based equalizer may be able to track this pattern and utilize the reflection constructively. The bottom-surface and surface-bottom reflections are clearly seen at about 2.5 ms.

The fading behaviour of the direct arrival was determined by estimating the signal strength of 100μs sections of the received signal using the ML estimator. Fig. 7 shows the fading of a single path as compared to Rayleigh fading. The observed fading is similar, but slightly better than Rayleigh. This fading probably occurs due to micro-multipath caused by suspended scatterers.

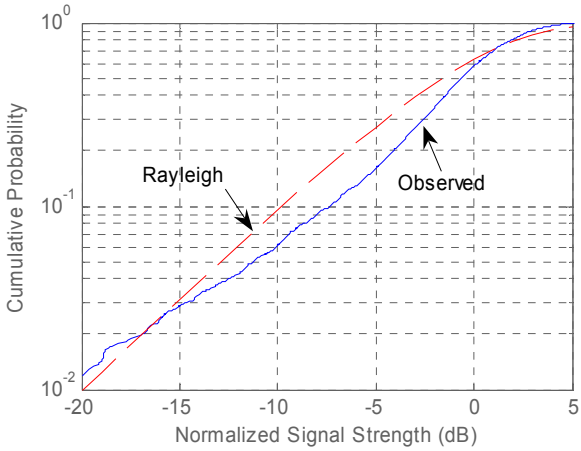

Fig. 7. Cumulative distribution function of signal strength showing fading behaviour of direct arrival at 50 m

2) Medium Range

The direct and surface reflected arrivals could not be independently resolved at medium range (550 m - 1020 m). The interference of the two arrivals led to a Lloyds' mirror effect causing a transmission loss increase as the 4th power of range [14]. However, the combined arrival could still be detected at 1020 m and the combined fading behaviour could be analyzed.

As seen in Fig. 8, the direct and surface reflected arrivals appear as a single arrival at 1020 m. The bottom reflected arrival is visible at about 0.08 ms. This arrival can be quite strong but is subject to severe fading. The signal strength appears to be slowly time-varying but the arrival time is quite stable compared to short range bottom arrival.

The stability of the arrival time is important for communication techniques utilizing equalization or time reversal mirrors (TRM). The time stability can be explained easily using a simple ray model. If R is the range, h_1 and h_2 are the heights of the transmitter and receiver above the sea bed, and c is the speed of sound, the arrival time difference is given by:

$$\tau = \frac{1}{c}\left[\sqrt{R^2 + h^2} - R\right] \qquad (4)$$
$$where\ h = h_1 + h_2$$

Assuming that the arrival time variability is due to the movement of the transmitter and receiver, we can explore the sensitivity of τ to changes in R and h.

$$\frac{\partial \tau}{\partial R} = \frac{1}{c}\left[\frac{R}{\sqrt{R^2 + h^2}} - 1\right]$$
$$\frac{\partial \tau}{\partial h} = \frac{1}{c} \cdot \frac{h}{\sqrt{R^2 + h^2}} \qquad (5)$$

In shallow waters, as the range increases, R >> h. Thus,

$$\frac{\partial \tau}{\partial R} \approx 0 \quad and \quad \frac{\partial \tau}{\partial h} \approx \frac{h}{cR} \qquad (6)$$

Hence, at longer ranges the arrival time difference is much less sensitive to movement of the transmitter and receiver. Even though reflections may demonstrate considerable time jitter at small ranges, they are relatively stable at medium to long ranges.

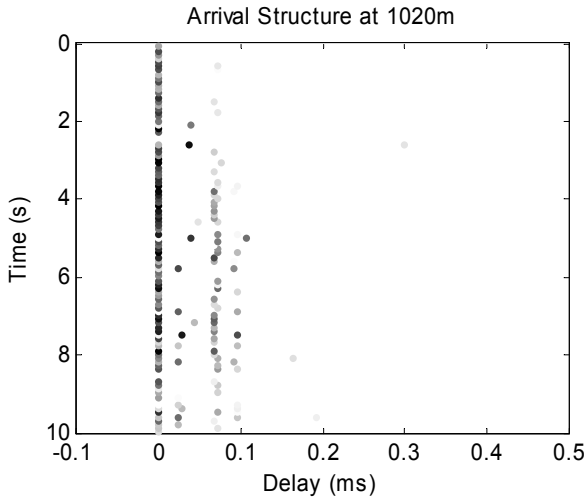

Fig. 8. Multipath arrival structure at 1020 m

The fading behaviour of the first arrival was determined by estimating the signal strength of 100μs sections of the received signal using the ML estimator. The first arrival consisted of the combined direct and surface reflected arrivals. A cumulative distribution plot of the fading is shown in Fig. 9. The first arrival exhibits much more fading than the Rayleigh distribution.

As the *first arrival* is formed by the interference of the direct and surface reflected arrival, one would expect that the fading could be explained as a function of the fading of each of the arrival. From short range measurements, we know that the direct arrival and surface reflected arrival are approximately Rayleigh distributed. As the time difference between the arrivals is very small, we may assume that the two arrivals interfere destructively. The resulting first arrival would then be distributed as the difference of two independent Rayleigh random variables.

We simulated the above model by subtracting two sets of 5,000 Rayleigh distributed random numbers and plotting the cumulative distribution function of the resulting magnitude. The simulation yielded an expected fading as shown in Fig. 10. The remarkable similarity in the simulated fading and the observed fading as shown in Fig. 9, suggest that the simple model suggested above is a good approximation of reality. A ray model with individual rays exhibiting independent Rayleigh fading explains both, the short and medium range data well.

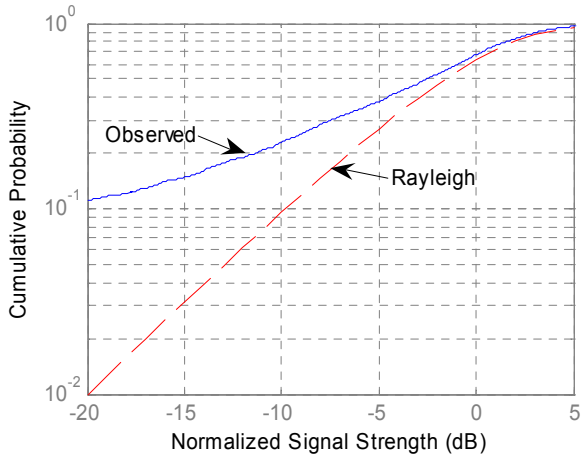

Fig. 9. Cumulative distribution function of signal strength showing fading behaviour of first arrival at 1020 m

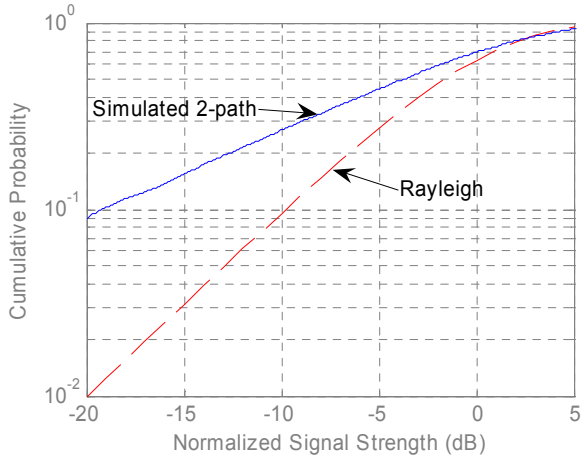

Fig. 10. Cumulative distribution function of Monte-Carlo simulation of 2-path fading

IV. CONCLUSIONS

Analysis of ambient noise in warm shallow waters clearly shows the non-Gaussian nature of the noise due to snapping shrimp. An SαS distribution fits the noise well and may be used as a noise model when designing detectors or communication systems to be operated in such waters. We demonstrated that a sign correlator is a near-optimal detector in snapping shrimp dominated noise. We also developed a ML estimator for signal strength in SαS noise.

With the tools developed for detection in non-Gaussian noise, we investigated the channel impulse response and time variability of a shallow water communication channel in Singapore. The results suggest that a ray model is a good approximation of the channel at high frequencies. At small range, there is significant variation in the impulse response due to movement of the transmitter and receiver. However, at medium to long range, the variation does not cause significant arrival time variation. The signal strength along each ray exhibits independent Rayleigh fading.

The simple Rayleigh fading ray model yields good agreement with data collected at ranges from 50 m to 1020 m. The fading statistics of interfering rays could also be explained with the model. Hence it may be used in the development of new communication systems to design model-based signal processing techniques. We expect that higher data rates and more reliable communication can be achieved in medium range shallow water channels with these techniques.

ACKNOWLEDGEMENTS

We would like to thank Mr. Koay Teong Beng who kindly made ambient noise available for analysis. We would also like to thank Dr. Paul Seekings, Mr. Koay Teong Beng and Mr. Mohan Panayamadam for their support during the sea trials. Dr. Paul Seekings and Mr. Shiraz S kindly reviewed the initial drafts of the paper, for which we are grateful.

REFERENCES

[1] Catipovic, Josko A., "Performance limitations in underwater acoustic telemetry," in IEEE J. Oceanic Eng. 15(3), pp.205-216, June 1990.

[2] Stojanovic, Milica, "Recent advances in high-speed underwater acoustic communications," in IEEE J. Oceanic Eng. 21(2), pp.125-136, April 1996.

[3] Stojanovic, Milica, Josko A. Catipovic and John G. Proakis, "Adaptive multi-channel combining and equalization for underwater acoustic communications," in J. Acoust. Soc. Am. 94, pp.1621-1631, 1993.

[4] Stojanovic, Milica, Josko A. Catipovic and John G. Proakis, "Phase-coherent digital communications for underwater acoustic channels," in IEEE J. Oceanic Eng. 19(1), pp.100-111, 1994.

[5] Kebkal, Konstantin G., Rudolf Bannasch, Alexey G. Kebkal and Sergey G. Yakovlev, "Ultrasonic link for improved incoherent data transmission in horizontal shallow water channels," in Proc. OCEANS 2003, USA, pp.1786-1792, September 2003.

[6] Potter J. R., Lim T. W. & Chitre M. A., “Ambient noise environments in shallow tropical seas and the implications for acoustic sensing”, Oceanology International 97, Singapore, 1997.

[7] Tan Soo Pieng, Koay Teong Beng, P. Venugopalan, Mandar A. Chitre and John R. Potter, "Development of a shallow water ambient noise database," in Proc. Underwater Technology 2004, Taiwan, April 2004.

[8] Verluis M., Schmitz B., Heydt A. & Lohse D., “How Snapping Shrimp Snap: Through Cavitating Bubbles,” in Science 289, pp.2114-2117, 2000.

[9] Kassam, Saleem A., "Signal detection in non-Gaussian noise," New York: Springer-Verlag, 1988.

[10] Nikias, Chrysostomos L. and Min Shao, "Signal processing with alpha-stable distributions and applications," New York: Wiley, 1995.

[11] McCulloch, J. H., "Simple consistent estimators of stable distribution parameters," in Comm. Stat. Sim., 15(4), pp.1109-1136, 1986.

[12] Fama, E. F. and R. Roll, "Parameter estimates for symmetric stable distributions," in J. Am. Stat. Assoc. 66, pp.331-338, 1971.

[13] McCulloch, J. Huston, "Numerical approximation of the symmetric stable distribution and density." in Robert J. Adler, Raisa E. Feldman and Murad S. Taqqu (Ed.), A practical guide to heavy tails. USA: Birkhäuser, 1998.

[14] Urick, Robert J., "Principles of underwater sound" (3rd edition), New York: McGraw-Hill, 1983.